A Broadband Optical Modulator Based on a Graphene Hybrid Plasmonic Waveguide

Xing Chen, Yue Wang, Yuanjiang Xiang, Guobao Jiang, Lingling Wang, Qiaoliang Bao, Han Zhang, Yong Liu, Shuangchun Wen, and Dianyuan Fan

***Abstract*—In this paper, a graphene hybrid plasmonic waveguide (HPW) modulator, in which a single layer of graphene-hexagonal-boron-nitride-graphene (graphene-hBN-graphene) has been embedded to enhance the absorption of the graphene, is numerically investigated based on a three-dimensional (3D) finite-difference time domain. The influences of geometric parameters, chemical potential, and dispersion on the fundamental mode of this modulator were determined. The height and width of the low index material results in significant effects to the effective mode index, which can determine the performance of the optical modulator. Using appropriate geometric parameter settings, this modulator could simultaneously offer a large extinction rate (up to 39.75 dB), broadband modulation bandwidth (up to 190.5 GHz), low power consumption (as low as 7.68 fJ/bit), and also provide subwavelength field confinement and long propagation distances. Wide-range wavelength response studies show that this optical modulator has good wavelength tolerance from 1200 to 1800 nm, indicating that it may be employed as an optical device exhibiting the desired performance. Furthermore, this optical modulator is not only suitable for optical fiber communications but also for free-space optical communications Our simulation results may provide experimental guidelines for designing future high-performance graphene optical modulators.**

***Index Terms*—Graphene, hybrid plasmonic waveguide (HPW), modulators, nanophotonics.**

Manuscript received December 9, 2015; revised August 7, 2016; accepted September 19, 2016. Date of publication September 21, 2016; date of current version October 13, 2016. This work was supported in part by the Natural Science Fund of China under Grant 61435010 and in part by the Science and Technology Innovation Commission of Shenzhen (KQTD2015032416270385 and JCYJ20150625103619275).

X. Chen and H. Zhang are with the Key Laboratory for Micro-Nano-Optoelectronic Devices of Ministry of Education, School of Physics and Electronics, Hunan University, Changsha 410082, China, and also with SZU-NUS Collaborative Innovation Center for Optoelectronic Science & Technology, and Key Laboratory of Optoelectronic Devices and Systems of Ministry of Education and Guangdong Province, Shenzhen University, Shenzhen 518060, China (e-mail: chenshin@hnu.edu.cn; hzhang@szu.edu.cn).

Y. Wang, G. Jiang, L. Wang, and S. Wen are with the Key Laboratory for Micro-Nano-Optoelectronic Devices of Ministry of Education, School of Physics and Electronics, Hunan University, Changsha 410082, China (e-mail: yuewang@hnu.edu.cn; andguobao@163.com; chenshin@live.cn; scwen@hnu.edu.cn).

Y. Xiang and D. Fan are with the SZU-NUS Collaborative Innovation Center for Optoelectronic Science and Technology, and Key Laboratory of Optoelectronic Devices and Systems of Ministry of Education and Guangdong Province, Shenzhen University, Shenzhen 518060, China (e-mail: xiangyuanjiang@126.com; dandy@cae.cn).

Q. Bao is with the Institute of Functional Nano and Soft Materials, Jiangsu Key Laboratory for Carbon-Based Functional Materials and Devices, and Collaborative Innovation Center of Suzhou Nano Science and Technology, Soochow University, Suzhou 215123, China (e-mail: qlbao@suda.edu.cn).

Y. Liu is with the State Key Laboratory of Electronic Thin Films and Integrated Devices, School of Optoelectronic Information, University of Electronic Science and Technology of China, Chengdu 610054, China (e-mail: yongliu@uestc.edu.cn).

Color versions of one or more of the figures in this paper are available online at http://ieeexplore.ieee.org.

Digital Object Identifier 10.1109/JLT.2016.2612400

I. Introduction

As, WHICH consists of a single layer of carbon atoms in a hexagonal lattice, has attracted a great deal of interest in the past decade due to its unique electronic and optical properties including broadband operation, ultrafast carrier relaxation, and relatively strong light-matter interactions [1]–[13]. Theoretically, graphene is considered a perfect atomic monolayer with infinite 2-D expansion with valence and conduction bands that slightly overlap at the Dirac point, making this material a unique zero-band-gap semiconductor [14]. Electron motilities at room temperature have been experimentally measured as high as 15000 $cm^2\ V^{-1}\ s^{-1}$ with very little temperature dependency and zero effective mass for the charge carriers [15]. The weak temperature dependency of the electron mobility of graphene suggests that electron movement is only limited by defect scattering other than phonon scattering, which commonly occurs in most materials. As a consequence, graphene possesses a theoretical resistivity limit of 10^{-6} Ωcm, making it one of the lowest resistance materials known at room temperature [16].

Wang *et al.* experimentally found that the strong inter-band transition in graphene could be substantially modified through electrical gating, similarly to electrical transport in field-effect transistors [17]. Such gate dependence on inter-band transitions introduces additional freedom in engineering new types of graphene-based, tunable optoelectronic devices, such as broadband optical detectors [18]–[20] and modulators [21], [22]. Consequently, its unique linear energy band and high carrier mobility at room temperature, in association with an optical transition that is controllable via an electrical gate, have made it widely applicable in electro-optic modulators from the visible to terahertz range [21]–[32]. Waveguide type electro-optical modulators based on single or double layer graphene schemes have been proposed [21]–[23]. However, these schemes suffer from the same issue: a low extinction rate (ER) due to the weaker interaction between the graphene and the evanescent electric field. However, schemes based on a ring resonator could achieve a higher ER, but with a fixed working wavelength, large footprint and higher energy consumption, rendering them very difficult to be implemented experimentally [24], [26]. Therefore, it is necessary to design a broadband, high ER, low consumption, multi-wavelength operable and small footprint modulator for use as a key element in next-generation electro-optic devices.

Hybrid plasmonic waveguides (HPWs) were proposed to simultaneously provide sub-wavelength field confinement and long propagation distances [33]–[41]. The HPWs usually consist of three individual layers: a high-index layer, a metal layer, and a low-index layer sandwiched between them [34], [36], and

[37]. The electric field will be highly confined in the high-index layer due to the index difference between the layers. This property provides a potential way to enhance the mutual interaction between the graphene and the electric field.

In this work, a HPW modulator based on graphene-hexagonal-boron-nitride-graphene (graphene-hBN-graphene) is proposed. The scheme for the graphene-hBN-graphene is embedded into a low-index layer of a HPW. The influence of the geometric parameters, chemical potential of the graphene and dispersion related to the fundamental mode (TM mode) of this modulator are studied in detail using a three-dimensional (3D) Finite-Difference Time-Domain (FDTD). The height of the low index material in the HPW and the width of the HPW have significant effects on the effective mode index (EMI). By optimizing these parameters, this electro-optical modulator can achieve an ER of up to 39.75 dB, a modulation bandwidth of 190.5 GHz with only a 3 μm long active region and a power consumption of 7.68 fJ/bit. This modulator can work over a wide wavelength range from 1200 nm to 1800 nm with advantages including a small footprint and easy fabrication.

II. Structure and Analysis

The conductivity of the graphene can be approximately reduced from the Kubo formalisms [6], [7] as follows:

$$\sigma(\omega) = \frac{2ie^2 k_B T}{\pi\hbar^2(\omega + i\tau^{-1})} \ln\left[2\cos h\left(\frac{\mu_c}{2k_B T}\right)\right] + \frac{e^2}{4\hbar}\left\{\frac{1}{2} + \frac{1}{\pi}\tan^{-1}\left(\frac{\hbar\omega - 2\mu_c}{2k_B T}\right) - \frac{i}{2\pi}\ln\left[\frac{(\hbar\omega + 2\mu_c)^2}{(\hbar\omega - 2\mu_c)^2 + (2k_B T)^2}\right]\right\}, \quad (1)$$

Where e is the charge of the electron, κ_B is the Boltzmann constant, T is the temperature, $\hbar$ is the reduced Planck constant, and ω is the angular frequency, and τ is the inter-band relaxation time. The chemical potential can be tuned via an applied voltage [17] of $\mu_c = \hbar\nu_F(\pi n_0)^{1/2} = \hbar\nu_F(\pi\varepsilon_0\varepsilon_r|V_g - V_{Dirac}|/de)^{1/2}$, where $v_F \approx 1.1 \times 10^6$ m/s is the Fermi velocity, n_0 is the carrier concentration in graphene, which can be determined from the simple parallel-capacitor model, V_g is the applied basis voltage and V_{Dirac} is the voltage offset caused by natural doping, d is the thickness of the hBN, e is the charge of the electron. Fig. 1 shows the permittivity of the graphene as a function of the chemical potential calculated from $\varepsilon(\omega) = 1 + i\sigma(\omega)/\varepsilon_0\omega d$ at $\lambda = 1550$ nm, where ε_0 is the permittivity in the vacuum and $d = 1$ nm, which is the equivalent thickness of monolayer graphene.

At approximately $\mu_c = 0.4$ eV, the real component of ε is maximized and its imaginary component starts to decrease to zero. At $\mu_c = 0.52$ eV, the absolute value of the permittivity approaches zero. When $\mu_c < 0.52$ eV, both the real and imaginary components are positive, meaning that the graphene operates as a dielectric material where the intra-band transmission dominates. However, the graphene shifts towards behaving like a metallic material when $\mu_c > 0.52$ eV due to the real component of ε becoming negative when the inter-band transmission dominates. Those changes manifest in the EMI of the modulator being correspondingly altered through the external electric field. Hence, it is necessary to investigate the EMI under different values of μ_c when designing an electro-optic modulator.

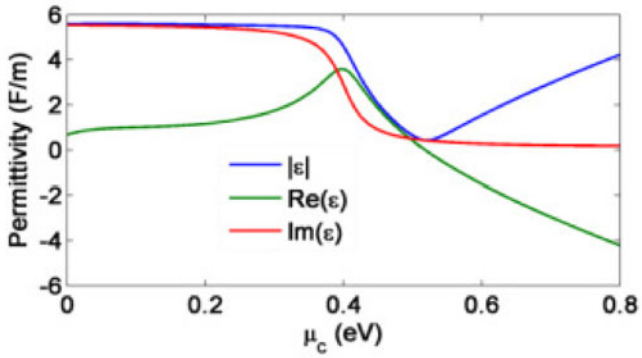

Fig. 1. The permittivity of graphene as a function of the chemical potential at $\lambda = 1550$ nm, where T = 300 K.

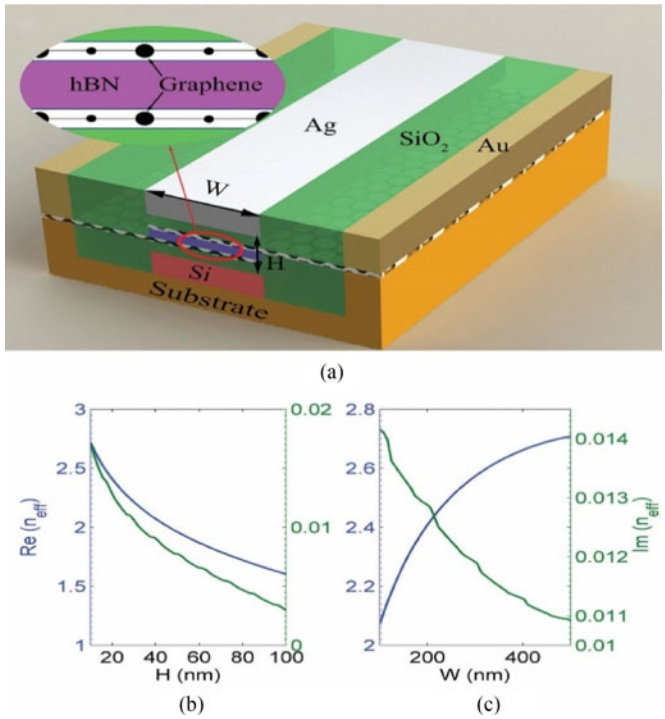

Fig. 2. (a) The scheme for the proposed modulator. The dependence of the EMI on (b) the height of the low-index layer and (c) the width of the HPW for $\lambda = 1550$ nm.

Fig. 2(a) shows the cross section of the as-proposed modulator. The HPW has a three layered structure, each with different indexes: a low index layer SiO_2 separated by the high index layer Si and metallic Ag. The graphene-hBN-graphene is embedded in the low index material layer of the HPW. The SiO_2 cladding is used to sustain the graphene layer and protect the graphene from optical or mechanical damage. The gold is used as the electrode where the external electric field can be applied. To determine the function of graphene-hBN-graphene layer, and therefore, compare the difference in performance, we first calculated the EMI for the HPW without the graphene-hBN-graphene layers.

We employed a 3-D FDTD commercial software (FDTD Solutions [42]) to evaluate the performance of this modulator. The refractive index of those materials (Ag - Palik, Si - Palik, SiO_2 - Palik) used in this study is taken from the FDTD Solutions directly which can well fit with the experimental data. The index of hBN is taken from ref. [43]. The mesh size in the thickness direction of graphene should be small enough. In our simulations, this value is 0.1 nm, while the other directions are set as 1 nm and 1 nm. The excitation source is the mode source. The boundary condition (BC) is set to perfectly matched layer (PML) with 48 layers. Note that the electrodes are not in the simulation area.

The height of the low-index layer (H) and the width of the HPW (W)play a central role in determining the EMI [34], [36] and [37], as shown in Fig. 2(b) and (c). The value of H increases from 10 nm to 100 nm, whereas the value of W is fixed at 200 nm. We see that a larger value of H can induce a lower imaginary component of the EMI, but with weaker mode confinement. However, a larger value of W has the opposite effect on the real component of the EMI compared to H: a larger value of W results in a larger real component in the EMI, whereas the imaginary component of the EMI exhibits the same trends as for H. This phenomenon can be easily understood from the effective index method point of view. The cross section of the HPW waveguide can be divided into three regions from left to right. The central region composed of $Ag/SiO_2/Si$ has a larger real index component than the left or right regions composed of SiO_2 cladding. The larger W leads to a larger contrast between the central region and other regions, whereas the contrast will determine the real component of the EMI. We can perform a similar analysis for H. Therefore, it is anticipated that this HPW will exhibit low losses and good mode confinement simultaneously, indicating that it can be used to fabricate a high performance modulator. In the following study, we consider the incorporation of a graphene-hBN-graphene layer that is sandwiched into the HPW. Then, we investigate the effect that different chemical potentials μ_c of the graphene and heights of the low-index layer have on the EMI. Here, the loss term, instead of the imaginary component of the EMI, is used for the visual presentation:

$$\text{Loss} = \frac{10\text{Im}\left(n_{eff}\right)4\pi}{\lambda_0 ln10} \tag{2}$$

where, λ_0 is the wavelength in free space, n_{eff} is defined as $n_{eff} = \beta\lambda_0/2\pi$, β is the propagation constant. The loss is proportionate to the imaginary component of the EMI. The height of the hBN layer is fixed at 5 nm for all the following calculations.

As shown in Fig. 3, different values of μ_c result in losses ranging from less than 1 dB/μm to more than 30 dB/μm, which suggests that this modulator will operate as expected. At approximately 0.525 eV, this modulator exhibits a minimum real component of EMI, but with a maximum loss. However, the real component of the EMI increases when μ_c is biased from that point. The loss trend is opposite of what was found in the real component of the EMI. The height H has a significant effect on the EMI, and it resembles the HPW. A smaller value of H has more advantages than a larger value. A thinner and smaller low-index layer will lead to a higher energy concentration, which

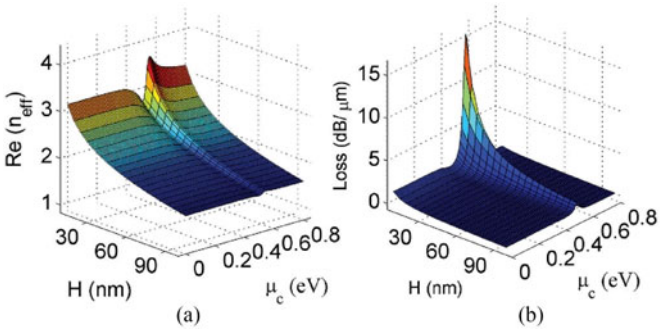

Fig. 3. Dependence of (a) the real component of EMI and (b) the losses on the H and μc, where W = 200 nm and λ = 1550 nm.

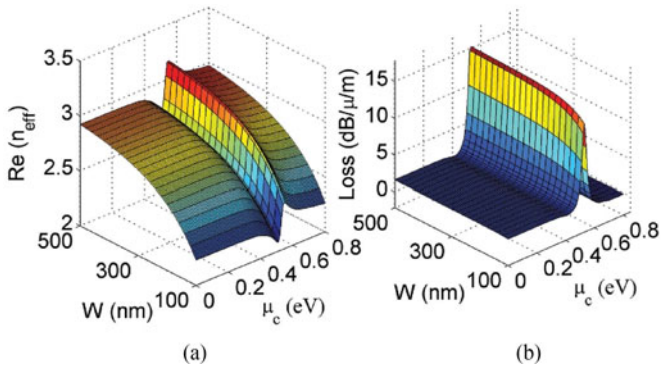

Fig. 4. Dependence of (a) the real component of the EMI and (b) the losses on the W and μc, where H = 20 nm and λ = 1550 nm.

TABLE I
OPERATION PERFORMANCE OF DIFFERENT TYPES OF OPTICAL MODULATORS

References	ER	3 dB Bandwidth	Consumption
This Study	13.75 dB/μm	190.5 GHz	7.68 fJ/bit
Ming Liu *et al.* [21]	0.1 dB/μm	1.2 GHz	NA
Ming Liu *et al.* [22]	0.16 dB/μm	~1 GHz	NA
Shengwei Ye *et al.* [23]	6.8 dB/μm	100 GHz	17.6 fJ/bit
Wei Du *et al.* [24]	22.13 dB	149 GHz	NA
CiyuanQiu *et al.* [45]	>10 dB	80 GHz	NA

will increase the interaction between the graphene and the electric field. Hence, it helps to increase the real component of the EMI [34], [37]. However, a small value of H makes the layers more difficult to fabricate, requiring us to take the fabrication error tolerance of the modulator into consideration. Based on the overall consideration of the various factors mentioned above, H = 20 nm was determined to be an appropriate height for this modulator. Moreover, our simulations show the position of graphene-hBN-graphene in the low-index layer cannot change the performance of the modulator.

We then investigated the effect of the HPW slab width on the EMI and losses. Fig. 4(a) shows the dependence of the real component of EMI on μ_c and W. Similarly to the HPW, W helps to improve the mode confinement and increase the ER. The losses in this optical modulator originate from: material absorption. A wider W will increase the absorption due to the expansion of the contact area, whereas the mode confinement will be greatly enhanced. Therefore, more energy is confined in the low-index

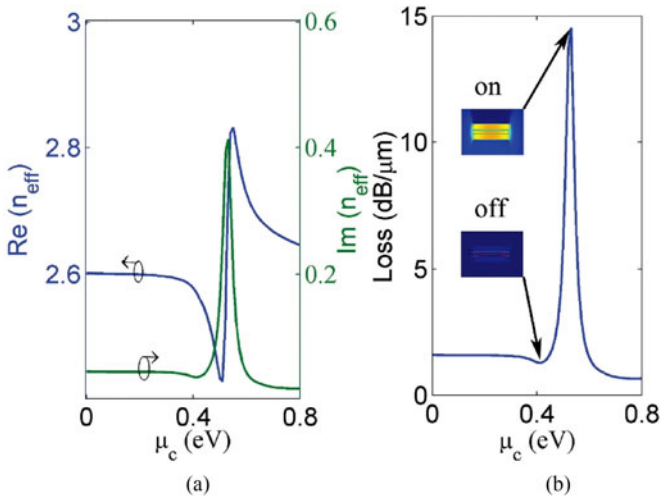

Fig. 5. (a) The real component of the EMI (blue line), the imaginary component of the EMI (green line), (b) the loss for the optimized modulator and electric field of the cross section in the modulator used for the insert, where W = 200 nm and H = 20 nm.

layer in contact with the graphene, leading to a higher value for ER. However, a wider W has a larger footprint, which is a disadvantage for nano-scale photonic integrated circuits (PLCs) and such an improvement is insufficient if W is larger than 200 nm. As discussed, W = 200 nm is an optimized value for the trade-off between the mode confinement and the footprint.

The imaginary and real components of the EMI and the losses for this modulator with the optimized geometric parameters are shown in Fig. 5. The losses are maximized at ~0.525 eV, indicating that this modulator suffers from large losses when light travels through it. Therefore, this point may be defined as the "off" state. The losses reach a minimum value at ~0.405 eV, which can be set as another working point, the "on" state. As previously mentioned, changing the applied voltage corresponds to a change in the chemical potential. This allows the optical modulator to operate in either the "off" or the "on" state. The voltage difference between the "off" and "on" states can be determined from $|\mu_c| = \hbar v_F(\pi n_0)^{1/2} = \hbar v_F(\pi\varepsilon_0\varepsilon_r|(V_g - V_{Dirac}|/de)^{1/2}$. In order to estimate the 3-dB modulation bandwidth and energy consumption, we used a simple parallel-capacitance model for calculation. The two layers of graphene are the two parallels of the capacitance, while the hBN is employed as the dielectric material. Hence, the chemical potential can be tuned via an applied voltage, $\mu_c = \hbar v_F(\pi n_0)^{1/2} = \hbar v_F\,(\pi\varepsilon_0\varepsilon_r|V_g - V_{Dirac}|/de)^{1/2}$, where $v_F \approx 1.1 \times 10^6$ m/s is the Fermi velocity, n_0 is the carrier concentration in graphene, V_g is the applied basis voltage, V_{Dirac} is the voltage offset caused by natural doping, ε_r is the dielectric constant of hBN and *d is* the thickness of hBN. The voltage difference ΔV between the "on" and "off" stage could be calculated from the equation mentioned above. The 3-dB modulation bandwidth is estimated by $\mathrm{f_{3dB}} = 1/(2\pi\mathrm{RC})$. The capacitance could be calculated by $\mathrm{C} = \varepsilon_0\varepsilon_r S/d$, where S (0.2 μm × 3 μm) is the area of capacitance. The resistance *R* comes from two sides: graphene-electrode contact resistance R_c and graphene sheet resistance R_g. However, the graphene sheet resistance is very small comparing with the contact resistance. Hence $\mathrm{f_{3dB}} = 1/(2\pi\mathrm{RC}) = 1/[2\pi(R_c + R_g)C] \approx 1/(2\pi R_c\mathrm{C})$, where we use $R_c = 400\,\Omega$ -μm as the contact resistance [44]. The energy consumption is calculated by $E_{bit} = \frac{1}{2}C(\frac{\sqrt{2}}{2}\Delta V)^2$, where *C* is the capacitance of this modulator, ΔV is the difference between the working point voltage. This modulator can achieve a 39.75 dB ER using only a 3 μm long active region. The estimated capacitance is *C* = 3.13 fF, and the variation in the voltage is $\Delta\mathrm{V} = 3.13$ V. The 3-dB modulator bandwidth is estimated to be 190.5 GHz, and the energy consumption is only 7.68 fJ/bit. Compared with other graphene-based optical modulators, the as-proposed modulator possesses better performance in some aspects. The following table lists some reported graphene-based modulators. Note that the last two references are for micro-ring based modulators, and therefore, the ER units are different from the others. Those improvements are the results of field enhancement, small contact resistance and small capacitance. The modulator based on the HPW can improve the interaction between the electric field and the graphene compared to Liu *et al.* [21], [22], in which the evanescent field was employed. Therefore, to improve the strength of the mutual interaction, multi-layer graphene needs to be used instead. Ye *et al.* embedded the graphene in the silicon waveguide to increase the interaction, leading to an ER of 6.8 dB μm [23]. However, stronger interactions can help achieve a higher 3-dB bandwidth with lower energy consumption. As discussed above, the 3-dB bandwidth is inversely proportional to the capacitance, whereas the power consumption is proportional to the capacitance. Hence, to achieve a high 3-dB bandwidth and a low energy consumption modulator, the capacitance needs to be sufficiently small.

Owing to the unique linear energy band structure in graphene, it exhibits broadband wavelength operations from the visible to the mid-infrared and even the microwave frequency range [2], [42], [43]. This property causes the graphene to act as a type of broadband optical material for different optical devices including a saturable absorber [48]–[50], optical detector [18]–[20], and optical modulator [21]–[26], [44]. To examine if the as-proposed graphene modulator could operate as a broadband device, we investigated the wavelength dependent response of the graphene-based optical modulator. The modulator possesses good mode confinement and operates from 1200 nm to 1800 nm, as shown in Figs. 6 and 7. With an increase in the operating frequency, the working point shifts towards the higher voltage regime because graphene has a higher shift point. The ER, ΔV and energy consumption decrease when the working wavelength shifts higher due to the permittivity properties of the graphene. However, the 3-dB modulation bandwidth is maintained at the same level due to the permittivity of the hBN being approximately constant over the wavelength range. These results demonstrate that our modulator has a relatively wide wavelength tolerance and could work over a wide wavelength range without changing anything except the applied bias voltage.

Graphene could achieve up to a 500 GHz 3-dB bandwidth in theory [21], which is more than twice that of ours. The consumption should be reduced to less than 1 fJ/bit in order

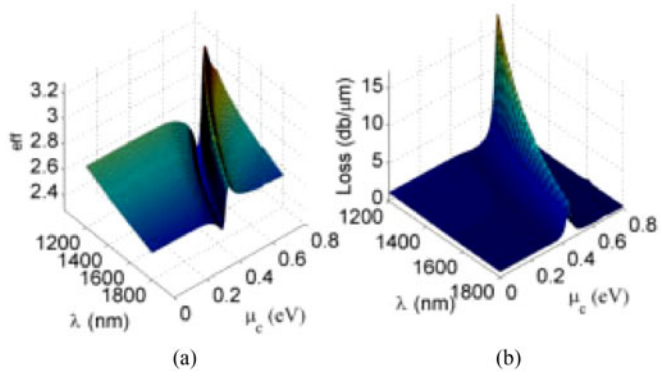

Fig. 6. Broadband wavelength operation: (a) real component of the EMI and (b) losses.

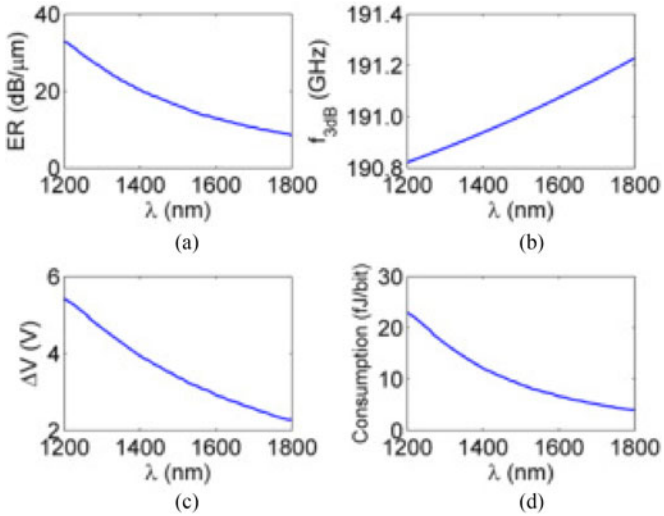

Fig. 7. The performance of the as-proposed optical modulator under broadband wavelength operation. (a)–(d) are ER, 3-dB modulation bandwidth, voltage difference between "OFF" and "ON," and energy consumption, respectively.

to integrate into high speed applications. A higher ER, higher bandwidth, lower consumption and smaller footprint may be appropriate future research goals for our program. By integrating hybrid plasmonic waveguides with other novel two-dimensional materials such as MoS_2 [51]–[53] and black phosphorus [54], [55], more functional devices with excellent performances may emerge and our work might contribute to the development of future 2D-material based optical modulators.

III. Conclusion

We have demonstrated a conceptual new optical modulator structure based on graphene and HWP as well as investigated its properties. Our simulations show that the geometric parameters of the HPW could significantly change the confinement mode and losses. By optimizing the width of the HPW and the height of the low-index layer in the HPW, this modulator could achieve a 39.75 dB extinction rate and a 190.5 GHz 3-dB modulator bandwidth with only a 3 μm long active region and 7.68 fJ/bit of energy consumption. Furthermore, this modulator can work over a wide wavelength range. Our work may offer new insight in designing high performance broadband optical modulators.

References

[1] K. S. Novoselov, "Electric field effect in atomically thin carbon films," *Science*, vol. 306, no. 5696, pp. 666–669, Oct. 2004.
[2] R. R. Nair *et al.*, "Fine structure constant defines visual transparency of graphene," *Science*, vol. 320, no. 5881, pp. 1308–1308, Jun. 2008.
[3] K. S. Novoselov *et al.*, "Two-dimensional gas of massless Dirac fermions in graphene," *Nature*, vol. 438, no. 7065, pp. 197–200, Nov. 2005.
[4] J. Wu, W. Pisula, and K. Mullen, "Graphene as potential material for electronics," *Chem. Rev.*, vol. 107, pp. 718–747, 2007.
[5] A. H. Castro Neto, N. M. R. Peres, K. S. Novoselov, A. K. Geim, and F. Guinea, "The electronic properties of graphene," *Rev. Modern Phys.*, vol. 81, no. 1, pp. 109–162, 2009.
[6] L. A. Falkovsky, "Optical properties of graphene," *J. Phys., Conf. Ser.*, vol. 29, 2008, Art. no. 012004.
[7] L. A. Falkovsky, "Optical properties of graphene and IV–VI semiconductors," *Phys.-Usp.*, vol. 178, no. 9, pp. 923–934, Sep. 2008.
[8] E. Hendry, P. J. Hale, J. Moger, A. K. Savchenko, and S. A. Mikhailov, "Coherent nonlinear optical response of graphene," *Phys. Rev. Lett.*, vol. 105, no. 9, Aug. 2010, Art. no. 097401.
[9] V. P. Gusynin, S. G. Sharapov, and J. P. Carbotte, "Anomalous absorption line in the magneto-optical response of graphene," *Phys. Rev. Lett.*, vol. 98, no. 15, Apr. 2007, Art. no. 157402.
[10] T. Otsuji *et al.*, "Graphene-based devices in terahertz science and technology," *J. Phys. D, Appl. Phys.*, vol. 45, 2012, Art. no. 303001.
[11] M. L. Nesterov, J. Bravo-Abad, A. Y. Nikitin, F. J. García-Vidal, and L. Martin-Moreno, "Graphene supports the propagation of subwavelength optical solitons," *Laser Photon. Rev.*, vol. 7, no. 2, pp. L7–L11, Mar. 2013.
[12] F. H. L. Koppens, D. E. Chang, and F. J. García de Abajo, "Graphene plasmonics: A platform for strong light–matter interactions," *Nano Lett.*, vol. 11, no. 8, pp. 3370–3377, Aug. 2011.
[13] J. C. Charlier, P. C. Eklund, J. Zhu, and A. C. Ferrari, "Electron and phonon properties of graphene: Their relationship with carbon nanotubes," *Top. Appl. Phys.*, vol. 111, pp. 673–709, 2008.
[14] K. S. Novoselov, "Nobel lecture: Graphene: materials in the flatland," *Rev. Modern Phys.*, vol. 83, no. 3, pp. 837–849, Aug. 2011.
[15] A. K. Geim and K. S. Novoselov, "The rise of graphene," *Nature Mater.*, vol. 6, no. 3, pp. 183–191, Mar. 2007.
[16] J.-H. Chen, C. Jang, S. Xiao, M. Ishigami, and M. S. Fuhrer, "Intrinsic and extrinsic performance limits of graphene devices on SiO_2," *Nature Nanotechnol.*, vol. 3, no. 4, pp. 206–209, Apr. 2008.
[17] F. Wang *et al.*, "Gate-variable optical transitions in graphene," *Science*, vol. 320, no. 5873, pp. 206–209, Apr. 2008.
[18] T. Mueller, F. Xia, and P. Avouris, "Graphene photodetectors for high-speed optical communications," *Nature Photon.*, vol. 4, pp. 297–301, 2010.
[19] L. Vicarelli *et al.*, "Graphene field-effect transistors as room-temperature terahertz detectors," *Nature Mater.*, vol. 11, no. 10, pp. 865–871, 2012.
[20] X. Yang, G. Liu, M. Rostami, A. A. Balandin, and K. Mohanram, "Graphene ambipolar multiplier phase detector," *IEEE Electron. Device Lett.*, vol. 32, no. 10, pp. 1328–1330, Oct. 2011.
[21] M. Liu *et al.*, "A graphene-based broadband optical modulator," *Nature*, vol. 474, no. 7349, pp. 64–67, 2011.
[22] M. Liu, X. Yin, and X. Zhang, "Double-layer graphene optical modulator," *Nano Lett.*, vol. 12, no. 3, pp. 1482–1485, Mar. 2012.
[23] S. Ye, Z. Wang, L. Tang, Y. Zhang, R. Lu, and Y. Liu, "Electro-absorption optical modulator using dual-graphene-on-graphene configuration," *Opt. Express*, vol. 22, no. 21, pp. 26173–26180, 2014.
[24] W. Du, E. Li, and R. Hao, "Tunability analysis of a graphene-embedded ring modulator," *IEEE Photon. Technol. Lett.*, vol. 26, no. 20, pp. 2008–2011, Oct. 2014.
[25] B. Sensale-Rodriguez, R. Yan, M. Zhu, D. Jena, L. Liu, and H. Grace Xing, "Efficient terahertz electro-absorption modulation employing graphene plasmonic structures," *Appl. Phys. Lett.*, vol. 101, no. 26, 2012, Art no. 261115.
[26] C. Qiu *et al.*, "Efficient modulation of 1.55 μm radiation with gated graphene on a silicon microring resonator," *Nano Lett.*, vol. 14, no. 12, pp. 6811–6815, Dec. 2014.
[27] B. Sensale-Rodriguez *et al.*, "Broadband graphene terahertz modulators enabled by intraband transitions," *Nature Commun.*, vol. 3, 2012, Art. no. 780.
[28] Y. Ding *et al.*, "Effective electro-optical modulation with high extinction ratio by a graphene–silicon microring resonator," *Nano Lett.*, vol. 15, no. 7, pp. 4393–4400, Jul. 2015.

[29] M. Mohsin *et al.*, "Experimental verification of electro-refractive phase modulation in graphene," *Sci. Rep.*, vol. 5, Jun. 2015, Art. no. 10967.
[30] A. Locatelli, G. E. Town, and C. De Angelis, "Graphene-based terahertz waveguide modulators," *IEEE Trans. THz Sci. Technol.*, vol. 5, no. 3, pp. 351–357, May 2015.
[31] Z. Lu and W. Zhao, "Nanoscale electro-optic modulators based on graphene-slot waveguides," *J. Opt. Soc. Amer. B*, vol. 29, no. 6, pp. 1490–1496, 2012.
[32] B. Sensale-Rodriguez *et al.*, "Extraordinary control of terahertz beam reflectance in graphene electro-absorption modulators," *Nano Lett.*, vol. 12, pp. 4518–4522, 2012.
[33] R. F. Oulton, V. J. Sorger, D. A. Genov, D. F. P. Pile, and X. Zhang, "A hybrid plasmonic waveguide for subwavelength confinement and long-range propagation," *Nature Photon.*, vol. 2, pp. 496–500, 2008.
[34] D. Dai and S. He, "A silicon-based hybrid plasmonic waveguide with a metal cap for a nano-scale light confinement," *Opt. Express*, vol. 17, no. 19, pp. 16646–16653, Sep. 2009.
[35] J. T. Kim, J. J. Ju, S. Park, M. Kim, S. K. Park, and S.-Y. Shin, "Hybrid plasmonic waveguide for low-loss lightwave guiding.," *Opt. Express*, vol. 18, no. 3, pp. 2808–2813, 2010.
[36] D. Dai, Y. Shi, S. He, L. Wosinski, and L. Thylen, "Gain enhancement in a hybrid plasmonic nano-waveguide with a low-index or high-index gain medium," *Opt. Express*, vol. 19, no. 14, pp. 12925–12936, 2011.
[37] M. Z. Alam, J. Meier, J. S. Aitchison, and M. Mojahedi, "Propagation characteristics of hybrid modes supported by metal-low-high index waveguides and bends," *Opt. Express*, vol. 18, no. 12, p. 12971–12979, Jun. 2010.
[38] K. Tanaka, M. Tanaka, and T. Sugiyama, "Simulation of practical nanometric optical circuits based on surface plasmon polariton gap waveguides," *Opt. Express*, vol. 13, no. 1, pp. 256–266, 2005.
[39] S. I. Bozhevolnyi, V. S. Volkov, E. Devaux, and T. W. Ebbesen, "Channel plasmon-polariton guiding by subwavelength metal grooves," *Phys. Rev. Lett.*, vol. 95, no. 4, Jul. 2005, Art. no. 046802.
[40] S. H. Chang, T. C. Chiu, and C.-Y. Tai, "Propagation characteristics of the supermode based on two coupled semi-infinite rib plasmonic waveguides," *Opt. Express*, vol. 15, no. 4, pp. 1755–1761, Feb. 2007.
[41] S. I. Bozhevolnyi, "Effective-index modeling of channel plasmon polaritons," *Opt. Express*, vol. 14, no. 20, pp. 9467–9476, 2006.
[42] FDTD Solutions. Lumerical Solutions, Inc., Canada. (2016). [Online]. Available: http:// www.lumerical.com
[43] A. Woessner *et al.*, "Highly confined low-loss plasmons in graphene–boron nitride heterostructures," *Nature Mater.*, vol. 14, no. 4, pp. 421–425, 2014.
[44] S. J. Koester and M. Li, "High-speed waveguide-coupled graphene-on-graphene optical modulators," *Appl. Phys. Lett.*, vol. 100, no. 17, 2012, Art no. 171107.
[45] C. Qiu, W. Gao, R. Vajtai, P. M. Ajayan, J. Kono, and Q. Xu, "Efficient modulation of 1.55 μm radiation with gated graphene on a silicon microring resonator," *Nano Lett.*, vol. 14, no. 12, pp. 6811–6815, Dec. 2014.
[46] K. F. Mak, M. Y. Sfeir, Y. Wu, C. H. Lui, J. A. Misewich, and T. F. Heinz, "Measurement of the optical conductivity of graphene," *Phys. Rev. Lett.*, vol. 101, no. 19, Nov. 2008, Art. no. 196405.
[47] J. M. Dawlaty, "Measurement of the optical absorption spectra of epitaxial graphene from terahertz to visible," *Appl. Phys. Lett.*, vol. 93, 2008, Art. no. 131905.
[48] Q. Bao *et al.*, "Atomic-layer graphene as a saturable absorber for ultrafast pulsed lasers," *Adv. Functional Mater.*, vol. 19, no. 19, pp. 3077–3083, Oct. 2009.
[49] G. X. Liu, D. J. Feng, M. S. Zhang, S. Z. Jiang, and C. Zhang, "Mode-locked erbium-doped all fiber laser using few-layer graphene as a saturable absorber," *Opt. Laser Technol.,* vol. 72, pp. 70–73, Sep. 2015.
[50] B. Gao, J. Huo, G. Wu, and X. Tian, "Soliton molecules in a fiber laser mode-locked by a graphene-based saturable absorber," *Laser Phys.*, vol. 25, no. 7, Jul. 2015, Art. no. 075103.
[51] J.-T. Liu, T.-B. Wang, X.-J. Li, and N.-H. Liu, "Enhanced absorption of monolayer MoS2 with resonant back reflector," *J. Appl. Phys.*, vol. 115, no. 19, May 2014, Art. no. 193511.
[52] Y. Li, C.-Y. Xu, B.-Y. Zhang, and L. Zhen, "Work function modulation of bilayer MoS2 nanoflake by backgate electric field effect," *Appl. Phys. Lett.,* vol. 103*,* no. 3*,* 2013, Art. no. 033122.
[53] B. Radisavljevic, A. Radenovic, J. Brivio, V. Giacometti, and A. Kis, "Single-layer MoS_2 transistors," *Nature Nanotechnol.*, vol. 6, no. 3, pp. 147–150, Mar. 2011.
[54] S. P. Koenig, R. A. Doganov, H. Schmidt, A. H. Castro Neto, and B. Özyilmaz, "Electric field effect in ultrathin black phosphorus," *Appl. Phys. Lett.*, vol. 104, no. 10, pp. 1–5, 2014.
[55] L. Li *et al.*, "Black phosphorus field-effect transistors," *Nature Nanotechnol.*, vol. 9, no. 5, pp. 372–377, Mar. 2014.

Authors' biographies not available at the time of publication.